Research Square

Preprints are preliminary reports that have not undergone peer review.
They should not be considered conclusive, used to inform clinical practice,
or referenced by the media as validated information.

Analysis of the Spatiotemporal Evolution of the Net Primary Productivity of Glycyrrhiza uralensis Fisch. and Its Influencing Factors from 2014- 2022

Xinxin Wei
Inner Mongolia University
Zeyuan Zhao
Inner Mongolia Traditional Chinese & Mongolian Medical Research Institute
Taiyang Chen
Inner Mongolia University
Xiaobo Zhang
National Resource Center for Chinese Materia Medica, China Academy of Chinese Medical Sciences
Minhui Li
Inner Mongolia Traditional Chinese & Mongolian Medical Research Institute
Tingting Shi
National Resource Center for Chinese Materia Medica, China Academy of Chinese Medical Sciences
Shuying Sun
nmgsunshuying@163.com
Inner Mongolia University

Article

Keywords: Glycyrrhiza uralensis Fisch., medicinal plants, Net primary productivity, carbon sequestration, GeoDetector

Posted Date: August 6th, 2025

DOI: https://doi.org/10.21203/rs.3.rs-7101862/v1

License: This work is licensed under a Creative Commons Attribution 4.0 International License.
Read Full License

Additional Declarations: No competing interests reported.

Article

Analysis of the Spatiotemporal Evolution of the Net Primary Productivity of *Glycyrrhiza uralensis* Fisch. and Its Influencing Factors from 2014- 2022

Xinxin Wei [1,2], Zeyuan Zhao [3], Taiyang Chen [1], Xiaobo Zhang [2], Minhui Li [3,*], Tingting Shi [2,*] , Shuying Sun [1,*]

[1] School of Life Sciences, Inner Mongolia University, Hohhot 010020, China; nmgsunshuying@163.com
[2] State Key Laboratory Breeding Base of Dao-di Herbs, National Resource Center for Chinese Materia Medica, China Academy of Chinese Medical Sciences, Beijing 100700, China; shitt@lreis.ac.cn
[3] Inner Mongolia Traditional Chinese & Mongolian Medical Research Institute, Hohhot 010010, China; prof_liminhui@yeah.net
* Correspondence: nmgsunshuying@163.com; prof_liminhui@yeah.net; shitt@lreis.ac.cn

Abstract: *Glycyrrhiza uralensis* Fisch. is widely used in medicine for its roots and rhizomes, and it plays a significant role in enhancing the regional ecological environment. In this study, firstly, based on the spectral characteristics of *G. uralensis* distribution areas under the *G. uralensis* Vegetation Index (GUVI) feature set of major feature types and *G. uralensis* in different years from 2014 to 2022, the *G. uralensis* distribution areas were identified and extracted using the Random Forest. Moreover, we estimated the Net Primary Productivity (NPP) of *G. uralensis* in Dengkou County using an improved version of the Carnegie-Ames-Stanford Approach (CASA) and investigated its spatio-temporal evolution characteristics. Additionally, with the assistance of GeoDetector, we systematically analyzed the relationship between the NPP of *G. uralensis* and 71 environmental factors from 2014 to 2022. The study findings indicated that the distribution area of *G. uralensis* fluctuated significantly over the years. Initially, its distribution was predominantly concentrated in the northeastern part of Dengkou County, but later it expanded to the southwestern region as well. Although the annual mean NPP of *G. uralensis* from 2014 to 2022 showed a fluctuating downward trend, it still accounted for a high proportion in the regions with high annual mean NPP within Dengkou County, which implies that *G. uralensis* has a strong carbon sequestration capacity. Furthermore, the GeoDetector analysis revealed that the impacts of various environmental factors on the spatial distribution of *G. uralensis* NPP in Dengkou County involve complex interaction relationships. This study offers valuable perspectives on the potential of *G. uralensis* as a key species for ecological restoration, desert management, sustainable utilization of medicinal plant resources, and carbon sequestration in (semi)arid regions. It also underscores the possibility of achieving a win-win situation for ecological conservation and economic development.

Keywords: *Glycyrrhiza uralensis* Fisch.; medicinal plants; Net primary productivity; carbon sequestration; GeoDetector

Academic Editor: Firstname Lastname

Received: date
Revised: date
Accepted: date
Published: date

Citation: To be added by editorial staff during production.

Copyright: © 2025 by the authors. Submitted for possible open access publication under the terms and conditions of the Creative Commons Attribution (CC BY) license (https://creativecommons.org/licenses/by/4.0/).

1. Introduction

With the rapid development of human society and the economy, a series of global ecological and environmental challenges have emerged, such as global warming, a drastic decline in forest area, and a substantial reduction in biodiversity. These issues present

significant challenges to humanity [1-3]. To tackle the ecological and environmental problems stemming from human activities [4], an increasing number of scholars have conducted in-depth investigations into the relationship between terrestrial ecosystems and global environmental change. Vegetation is of crucial significance in ecosystems [5, 6]. Its dynamic changes are closely associated with the stability and security of these systems. Conversely, the type, quantity, and quality of vegetation are significantly influenced by climate change and human activities [7]. Therefore, monitoring vegetation dynamics and studying their responses to environmental factors are of critical importance [8].

Medicinal plants, as an important component of diverse vegetation types, not only provide medicinal value for disease treatment but also play significant ecological roles, such as enhancing soil quality and preventing soil erosion. Nevertheless, previous research has mainly concentrated on their economic value [9, 10], often neglecting their ecological value [11-13]. Edo et al. conducted an investigation into the socio-ecological benefits of home garden agroforestry and its indigenous management system in Digelu Tijo Zone, Ethiopia, and showed that the percentage of social use categories of these plants, from the largest to the smallest, were edible plants, medicinal plants, fodder plants, construction plants, income generating plants, ornamental plants, spice plants, and shade plants, among others. Their ecological values include maintaining soil fertility, providing habitat for many organisms, improving water quality, preventing soil erosion, carbon sequestration, and improving soil moisture through shading. These plants are of great importance for food security and the restoration of ecosystem services, especially in devastated areas. The potential of different plant species to offer multiple uses and a wide array of ecological goods and services far exceeds what has been previously recognized[14]. In addition, scholars [15, 16]have reported that medicinal plants store significant amounts of carbon, which can enhance soil organic carbon content, improve soil fertility, increase agricultural yield, and reduce greenhouse gas emissions. These contributions are of great significance in promoting the development of sustainable ecosystems. Particularly for (semi) arid areas, where economic development is hindered by the decline or loss of biological and economic productivity caused by land degradation, cultivating crops with both ecological and economic value offers a vital pathway to breaking the cycle of degradation and achieving a sustainable ecological and economic balance. In an attempt to find a sustainable, profitable and effective method of CO2 capture, Ghazzawy, HS et al conducted an in-depth assessment of the ability of paulownia trees to capture atmospheric CO2, which showed that paulownia trees have ornamental, cultural and medicinal value, as well as strong carbon sequestration capacity and broad environmental suitability for use in agroforestry systems, and that large-scale planting is expected to meet global climate goals by 2050[17]. Chen et al studied the carbon sequestration and oxygen release capacity of 10 typical plants in the Helan Mountains, which is a transition zone between the temperate grassland area and the desert area in China[18]. They showed that the carbon sequestration and oxygen release capacity of *Picea crassifolia* Kom., *Populus davidiana* Dode, *Cotoneaster hissaricus* Wall. ex Lindl., and *Thermopsis lanceolata* R. Br. were all strong. And all these plants can be used as medicine. Lucía Andreu-Coll et al explored the fresh food production and non-food uses of Opuntia in countries such as Mexico, Italy and Spain (exploiting its biofunctional, medicinal, nutraceutical and cosmetic properties) and environmental mitigation of climate change through soil carbon sequestration are explored[19]. Ultimately it was shown that this crop is usually grown in more rural areas by smallholders and micro-farmers. Opuntia cultivation can be an effective means for rural development in (semi -)arid regions of Europe, covering aspects such as production, job creation, and environmental protection. Therefore, considering the unique characteristics of (semi -)arid ecosystems, we should search for plants with high economic and ecological value that are adaptable to (semi -)arid agro-ecosystems. This will offer more alternatives

for achieving the dual goals of maximizing ecological restoration and economic development in (semi -)arid areas, which is of great significance for multiple reasons.

Glycyrrhiza uralensis Fisch., a plant of the genus Glycyrrhiza in the Leguminosae family, is used medicinally based on its roots and rhizomes, which exhibit analgesic, cough suppressant, anti-inflammatory, anti-ulcer, and anti-allergic properties. It is widely utilized in various fields, including medicine, food, and cosmetics [20-24]. As a perennial leguminous plant, *G. uralensis* features a well-developed root system, high tolerance to light and drought, and strong resistance to adverse conditions. In arid and semi-arid regions, it plays a vital role in ecological protection, acting as windbreaks and facilitating sand fixation. Moreover, it is a key wild sand-fixing plant under the protection and management of China [25]. In recent years, due to the growth of market demand for *G. uralensis*, people's predatory digging, and local agricultural development, among other reasons, the fluctuation in the *G. uralensis* planting area has become more pronounced. Consequently, the utilization of modern information technology for *G. uralensis* identification has become a necessary initiative to promote the sustainable development of the *G. uralensis* planting industry and to formulate a development plan for local agriculture. Remote sensing technology, as an emerging information acquisition method, has been widely employed in agricultural production due to its timeliness, large-scale synchronous observation capability, and other advantageous characteristics. It plays a crucial role in the investigation and assessment of plant resources, growth monitoring and prediction, ecological environment monitoring and assessment, as well as precision agriculture and management [26-28]. Therefore, the use of remote sensing technology to identify the distribution area of *G. uralensis* not only enhances our understanding of the distribution and growth status of *G. uralensis* resources but also provides a scientific basis and technical support for their rational utilization and ecological protection.

In summary, medicinal plants play a vital role in the ecosystem. Their existence and functions are crucial for maintaining ecological equilibrium and promoting economic development. *G. uralensis*, as a medicinal plant with diverse applications, also contributes significantly to conserving groundwater resources, preventing land sandification, and enhancing the regional ecological environment, thanks to its well-developed root system. Understanding the ecological value of *G. uralensis* is conducive to the rational planning of *G. uralensis* cultivation, which helps to achieve ecosystem balance and ensure the long-term supply of *G. uralensis* resources. Therefore, in this study, *G. uralensis* was selected as the research object, and Dengkou County, which has a long-standing cultivation history and rich experience in the (semi-)arid region, was chosen as the study area. The distribution areas of *G. uralensis* were identified and extracted using the random forest (RF)model based on the images from the wide-field-view of the Gaofen-1 satellite (GF-1 WFV). Subsequently, the improved CASA model was employed to estimate and analyze the spatial and temporal variations of *G. uralensis* Net Primary Productivity (NPP) in Dengkou County from 2014 to 2022, incorporating remote sensing images and meteorological data. Finally, GeoDetector was employed to analyze the relationship between NPP of *G. uralensis* and 71 environmental factors in Dengkou County from 2014 to 2022, aiming to identify the key drivers influencing NPP of *G. uralensis* during this period. This study provides an important reference for selecting *G. uralensis* as a key species for ecological restoration, desert management, sustainable utilization of medicinal plant resources, and carbon sequestration in (semi-)arid regions, thereby facilitating a win-win situation for ecological construction and economic development.

2. Materials and Methods

2.1. Study area

Dengkou County is located in the western part of Inner Mongolia Autonomous Region, within Bayannur City. As shown in Figure 1, it is located at the convergence zone between the river-bend plain and the Ulanbuh Desert. The county has a highest elevation of approximately 1951 m above sea level and a total area of about 4,200 km². Its topography and geological features are diverse, mainly consisting of sandy areas, mountains, and plains, earning it the reputation of "seven-sands, two-mountains, and one-plain." It is one of the nine experimental demonstration counties for sand control and prevention in China. The county experiences a temperate continental monsoon climate, characterized by short springs and autumns, long cold winters, and hot summers. The average annual temperature is around 9.16 °C; the average annual rainfall ranges from 106 to 155 mm; the diurnal temperature difference is relatively large, approximately 14.5 °C; and the frost-free period lasts from 136 to 144 days. These conditions endow the county with unique foundations and conditions for developing modern agriculture and animal husbandry. In addition to traditional crops like *Zea mays* L. and *Glycine max* (L.) Merr., the planting areas of medicinal plants such as *Cistanche deserticola* Ma, *G. uralensis*, and *Astragalus membranaceus* (Fisch.) Bunge have been increasing year by year in recent years. Moreover, as part of the "two-screens and three-belts" ecological security strategy pattern, Dengkou County shoulders three crucial tasks: protecting the Yellow River, lakes, wetlands, and water systems within the county; preventing the further expansion of the Ulanbuh Desert; and conducting the comprehensive management of Wuliangsu Sea. Therefore, it is in the core position of the "Northern Sand Prevention Belt" [29, 30].

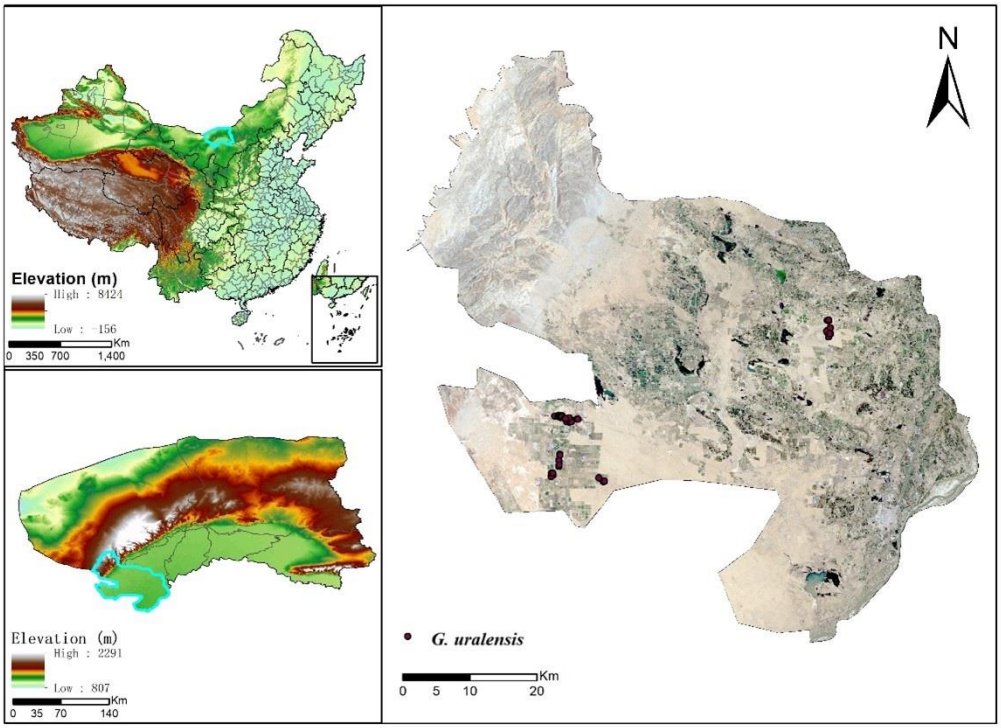


Figure 1 *G. uralensis* sample sites and their image maps in Dengkou County

2.2. Data sources and pre-processing

2.2.1. Remote sensing image

The remote-sensing image data utilized for identifying *G. uralensis* in this study were sourced from the Gaofen-1 Satellite Wide Field of View (GF-1 WFV) image. This data is freely accessible through the Land Observing Satellite Data Service of the China Centre for Resources Satellite Data and Application (https://data.cresda.cn/#/home). The

technical indicators of the payload are presented in Table 1. The GF-1 satellite was launched relatively early. It features higher spatial resolution, a wider swath width, and a shorter revisit period [31]. As a result, a larger amount of historical image data can be acquired. The details in these images are clearer, covering more information, and within the same time frame, more image data can be obtained.

For the acquired GF-1 WFV images, the following pre-processing steps were implemented. First, the WFV data were radiometrically calibrated using the absolute radiometric calibration coefficients of GF-1 for the same period released by the China Resource Satellite Application Centre. Subsequently, the GF-1 WFV spectral response function was imported into the spectral library file, and atmospheric correction was implemented via the FLAASH module. Finally, ortho-correction was performed on the images using GMTED2010 elevation data. After undergoing radiometric calibration, atmospheric correction, and ortho-correction, the data can, to a certain degree, reduce the atmospheric influence and achieve high geometric accuracy. This enables better registration of multi-period images.

Table 1. GF-1 WFV satellite payload technical specifications

Satellite data	Band	Wavelength (mm)	Band Description	spatial resolution (m)	Span (Km)	Revisit cycle (days)
GF-1 WFV	Band 1	450-520	blue band	16	800	2
	Band 2	520-590	green band			
	Band 3	630-690	red band			
	Band 4	770-890	near infrared (NIR)			

2.2.2. NDVI data

The NDVI data was derived from a comprehensive processing pipeline involving preprocessing, mosaicking, cropping, and index calculation applied to 172 GF-1 WFV remote sensing images spanning the period from 2014 to 2022.

2.2.3. Temperature and precipitation data

Monthly average temperature and monthly total precipitation data for each month from January to December during the 2014 - 2022 period, which were obtained from meteorological observatories around Dengkou County, were sourced from the National Oceanic and Atmospheric Administration (NOAA) U.S. National Centers for Environmental Information (NCEI, https://www.ncei.noaa.gov). Monthly total solar radiation data were obtained from the Data and Information Services Centre (DISC) of the Goddard Earth Sciences (GES) at the National Aeronautics and Space Administration (NASA) in the United States of America.

2.2.4. Vegetation type data

Vegetation type data were classified into five categories, namely woodland, desert, wetland, cropland, and others, based on field observations and visual interpretation of remotely sensed imagery. These data were obtained by classifying the 2014-2022 GF-1 WFV data using the RF algorithm.

2.2.5. MOD17A3HGF product data

The 2014-2022 MOD17A3HGF product data were obtained from NASA (https://ladsweb.modaps.eosdis.nasa.gov/). The MOD17A3HGFNPP data represent annual values

with a resolution of 500 m, and this NPP data is the sum of the values of the year's MOD17A2H product.. The NPP is estimated by the coupled model of PSN and BIOME-BGC. This model has successfully estimated the spatial and temporal variations of NPP in global ecosystems and has been validated and widely applied in studies related to the evaluation of different vegetation growth conditions, environmental monitoring, and carbon cycle research.

2.2.6. Environmental factor

In this study, a total of 71 environmental factor data with a resolution of 1 km were utilized. These data were obtained from the "Grid Database of Spatial Information on Traditional Chinese Medicine Resources" (http://www.tcm-resources.com/), as presented in Table 2. After importing the data into ArcMap, 100 points were randomly generated based on the distribution of *G. uralensis*, and the data were extracted to these random sampling points. Subsequently, GeoDetectors were employed to obtain the factor detection, interaction detection, and ecological detection for the relationships between the environmental factors and the NPP of *G. uralensis* in Dengkou County.

Table 2. Environmental factor data

Number	Name	Number	Name
X1	Wettest season average temperature	X37	Average growing season temperature
X2	Wettest season precipitation	X38	Average temperature in 4
X3	Precipitation in the driest season	X39	Average temperature in 3
X4	Average temperature of the driest season	X40	Average temperature in 2
X5	Monthly average of diurnal temperature difference	X41	Average temperature in 12
X6	Warmest Month Maximum Temperature	X42	Average temperature in 9
X7	Standard deviation of seasonal variations in temperature	X43	Average temperature in 11
X8	Warmest season average temperature	X44	Average temperature in 8
X9	average annual temperature	X45	Average temperature in 10
X10	Warmest season precipitation	X46	Average temperature in 7
X11	Range of mean annual temperature variations	X47	Average temperature in 1
X12	Lowest temperature of the coldest month	X48	Average temperature in 6
X13	Average annual precipitation	X49	Average sunshine hours in 6
X14	Average temperature of the coldest season	X50	Average sunshine hours in 5
X15	Coefficient of variation of seasonal precipitation	X51	Average sunshine hours in 4
X16	Coldest season precipitation	X52	Average sunshine hours in 3
X17	Isothermal	X53	Average sunshine hours in 2
X18	Dryest Monthly Precipitation	X54	Hours of sunshine during the growing season
X19	Wettest Monthly Precipitation	X55	Average sunshine hours in 1
X20	Slope	X56	Annual sunshine hours
X21	Aspect	X57	Average sunshine hours in 12
X22	Altitude	X58	Average sunshine hours in 9
X23	Precipitation in 5	X59	Average sunshine hours in 11
X24	Growing season precipitation	X60	Average sunshine hours in 8
X25	Precipitation in 4	X61	Average sunshine hours in 10
X26	Precipitation in 3	X62	Average sunshine hours in 7
X27	Precipitation in 2	X63	Organic carbon content
X28	Precipitation in 12	X64	Soil texture classification
X29	Precipitation in 9	X65	Soil effective water content class
X30	Precipitation in 11	X66	Soil subclass
X31	Precipitation in 8	X67	Cation exchange capacity of the soil
X32	Precipitation in 10	X68	Acidity and alkalinity (pH)
X33	Precipitation in 7	X69	Clay content of soil
X34	Precipitation in 1	X70	Soil sand content
X35	Precipitation in 6	X71	Vegetation type
X36	Average temperature in 5		

2.3. Methods

2.3.1. Random forest

Random forest (RF) is an ensemble learning algorithm that classifies and predicts samples by training multiple decision trees. Two key parameters are of crucial importance in the RF: the number of decision trees and the number of split nodes in each tree. By training, classifying, and predicting the data using multiple decision trees, the RF can fully utilize the differences between different trees, thus improving the accuracy and stability of classification. Additionally, the RF effectively reduces the errors that might be

generated by a single classifier through the method of voting classification by multiple classifiers, which further enhances the reliability of classification. As a novel machine learning algorithm, the random forest algorithm shows significant advantages in the field of remote sensing classification. It is capable of integrating numerous decision trees to generate classification results with higher accuracy [32].

In this study, four different metrics, namely Overall Accuracy (OA), Kappa coefficient (KC), Producer's Accuracy (PA), and User's Accuracy (UA), were utilized to comprehensively evaluate the classification results [33]. OA refers to the ratio of the total number of correctly classified image elements to the total number of image elements. The KC is an index of consistency testing. While OA can directly reflect the proportion of correct classification and is simple to calculate. However, due to sample imbalance during the classification process, the accuracy of some categories may be very low even when the OA value is high, and the KC can reflect this issue. Specifically, if one category has a poor classification result, the KC value will be significantly reduced. PA is the ratio of the total number of pixels correctly classified into a category by the classifier to the total number of actual references in that category, indicating the probability of correct classification for a category. A higher PA value implies less under-classification of the actual category. UA is the ratio of the total number of pixels correctly classified into a category to the total number of pixels classified into that category, indicating the probability of correctly classifying a category. A higher UA value indicates less misclassification in the classification result. The evaluation metric formulas described above are shown in Equations 1-4:

$$OA = \frac{\sum_{i=1}^{r} x_{ii}}{N} \quad (1)$$

$$Kappa = \frac{N \cdot \sum_{i=1}^{r} x_{ii} - \sum_{i=1}^{r} (x_{i+} \cdot x_{+i})}{N^2 - \sum_{i=1}^{r} (x_{i+} \cdot x_{+i})} \quad (2)$$

$$PA = \frac{x_{ii}}{x_{+i}} \quad (3)$$

$$UA = \frac{x_{ii}}{x_{i+}} \quad (4)$$

where N is the total number of reference sample points or the total number of reference pixels, r is the number of rows or columns of the error matrix, x_{ii} is the number of a category on the main diagonal of the matrix, and x_{i+} and x_{+i} are the number of samples in the ith row and the ith column, respectively.

2.3.2. CASA model

The CASA (Carnegie-Ames-Stanford Approach) model is a typical light energy utilization model driven by a combination of remotely sensed, meteorological, vegetation and soil type data, which takes into account the internal factors of the plant and the environment in which it is located on its NPP [34-36]. The vegetation NPP is mainly estimated by the product of the photosynthetically active radiation (APAR) absorbed by the vegetation and the vegetation light energy utilization (ε) together, as shown in Equation 5:

$$NPP(x,t) = APAR(x,t) \times \varepsilon(x,t) \quad (5)$$

where x denotes the geographical location; t denotes the month; APAR (x, t) denotes the photosynthetically active radiation absorbed by vegetation at image x in the month of t (MJ•m^{-2}•month^{-1}); ε (x, t) denotes the actual light energy utilization rate of vegetation at image x in the month of t (gC •MJ^{-1}). APAR and ε are calculated as shown in Equations 6 and 7:

$$APAR(x,t) = 0.5 \times SOL(x,t) \times FPAR(x,t) \quad (6)$$

$$\varepsilon(x,t) = T_{\varepsilon 1}(x,t) \times T_{\varepsilon 2}(x,t) \times W_{\varepsilon}(x,t) \times \varepsilon_{max} \quad (7)$$

Where, SOL(x, t) denotes the total solar radiation (MJ•m^{-2} month^{-1}) at pixel x in month t. FPAR(x, t) denotes the absorption ratio of incident solar photosynthetically active radiation (SAPAR) by the vegetation layer at spatial x. 0.5 is the ratio of the solar

active radiation utilized by vegetation to the total radiation. ε(x, t)is the efficiency of the SAPAR absorbed by the plants to be converted into organic carbon. $T_{\varepsilon 1}(x,t)$, $T_{\varepsilon 2}(x,t)$ are the extent to which the net primary productivity of the plant is reduced by the physiological effects of low or high temperatures that result in a limitation of photosynthesis. The energy utilisation of $T_{\varepsilon 2}(x,t)$ tends to decrease when the optimum growth temperature shifts towards higher and lower temperatures. $W_{\varepsilon}(x,t)$ is the extent to which the water state is the limit of light energy utilisation efficiency. ε_{max} is the maximum light energy utilisation under ideal conditions.

The validation of NPP values can be performed by two methods: the measured value validation method and the relative validation method. Due to the lack of measured data, this study used an indirect validation method to compare the CASA model NPP inversion results with MOD17A3HGF NPP data. Therefore, in this study, 30 points were randomly generated in the study area, from which MOD17A3HGF NPP values and NPP results estimated by CASA model were extracted to validate the model's estimation of NPP in Dengkou County. The coefficient of determination (R^2) and root mean square error (RMSE) were used in this study to measure the accuracy of the CASA model [37, 38].As shown in Equation 8 and 9:

$$R^2 = \frac{Cov(Y_t, Y_p)}{\sigma Y_t \sigma Y_p} \quad (8)$$

$$RMSE = \sqrt{\frac{\sum(Y_t - Y_p)^2}{N}} \quad (9)$$

where Y_t is the MOD17A3 NPP value for the nth random sample point and Y_p is the NPP value for the nth random sample point estimated using the CASA model.

2.3.3. GeoDetector

GeoDetector is a test of the spatial distribution of variables, and the GeoDetector software used in this study was downloaded from the GeoDetector official website (geodetector.cn/). GeoDetector is a statistical method for revealing potential drivers, and there are four detectors: factor detection, interaction detection, ecological detection, and risk detection [39-41]. This study focuses on exploring the influencing factors behind the change in NPP of *G. uralensis* in Dengkou County from 2014-2022 using GeoDetector.

(1) Factor detection

The factor detector quantitatively measures the spatial stratified heterogeneity (SSH) of each environmental factor on the spatial distribution of *G. uralensis* NPP in Dengkou County mainly through the magnitude of factor explanatory power. The factor explanatory power is the q value, which ranges from [0, 1]. The larger q value indicates that the factor has stronger explanatory power on the spatial distribution of NPP, q=0 indicates that the factor does not have any relationship with NPP, and q=1 indicates that the factor can completely explain the spatial distribution of NPP. As shown in Equation 10:

$$q = 1 - \frac{1}{N\partial^2}\sum_{i=1}^{L} N_i \partial_i^2 \quad (10)$$

Where q is a factor detection measure, which indicates the magnitude of the influence of an environmental factor on the spatial and temporal distribution of NPP; L is the number of samples of the environmental factor, N_i is the NPP in stratum i, N is the NPP in the whole study area, ∂_i^2 is the dispersion variance of the NPP in stratum i, and ∂^2 is the dispersion variance of the NPP in the whole study area.

(2) Interaction detection

It can be used to identify the interaction effect of two influence factors X1 and X2 superimposed on *G. uralensis* NPP in Dengkou County. When assessing the interaction of two factors, the sum of the PD values of the two factors and the PD value of the two-factor interaction was used to judge whether their degree of action on *G. uralensis* NPP was

increased or decreased, or the two factors acted independently, and the specific judgement was shown in Table 3.

Table 3. GeoDetector interaction relationships

Basis of judgement	interactive relationship
q(X1∩X2)＜Min(q(X1),q(X2))	Weaken, nonlinear
Min(q(X1),q(X2))＜q(X1∩X2)＜Max(q(X1),q(X2))	Weaken, uni-
q(X1∩X2)＞Max(q(X1),q(X2))	Enhance, bi-
q(X1∩X2)＝q(X1)＋q(X2)	Independent
q(X1∩X2)＞q(X1)＋q(X2)	Enhance, nonlinear

* Min(q(X1),q(X2)) means taking the minimum value of q(X1) and q(X2). q(X1)+q(X2) is the sum of q(X1) and q(X2). Max(q(X1),q(X2)) means to take the maximum value of both q(X1) and q(X2). q(X1∩X2) means that q(X1) and q(X2) interact with each other.

(3) Ecological detection

The F statistic was used to compare whether there was a significant difference between the effects of two environmental factors X1 and X2 on the spatial distribution of *G. uralensis* NPP in Dengkou County. The formula is 11:

$$F = \frac{N_{X1} \times (N_{X2} - 1) \times SSW_{X1}}{N_{X2} \times (N_{X1} - 1) \times SSW_{X2}} \quad (11)$$

SSW_X1 and SSW_X2 are calculated as follows Equation 12 and 13:

$$SSW_{X1} = \sum_{i=1}^{L_1} N_i \partial_i^2 \quad (12)$$

$$SSW_{X2} = \sum_{i=1}^{L_2} N_i \partial_i^2 \quad (13)$$

Where: N_{X1} and N_{X2} are the number of samples of environmental factors X1 and X2, respectively; SSW_{X1} and SSW_{X2} denote the sum of the intra-stratum variances of the strata formed by X1 and X2, respectively; and L1 and L2 denote the number of strata of variables X1 and X2, respectively. Where the null hypothesis H0: $SSW_{X1} = SSW_{X2}$, if H0 is rejected at the significance level of α, it indicates that there is a significant difference between the effects of the two factors X1 and X2 on the spatial distribution of *G. uralensis* NPP.

3. Results

3.1. Dynamic monitoring of G. uralensis range

After preprocessing the remote sensing images from 2014 to 2022, the *G. uralensis* vegetation index (GUVI) was calculated for each month's image, and the GUVI of different years was combined into nine feature sets of the RF algorithm in the order of January-December and according to the different growth years of *G. uralensis*. In addition to other feature types of spectral curve interpretation features and visual interpretation obtained from 2014 to 2022 historical images of *G. uralensis* and other feature types, after selecting the training set and validation set in the ratio of 7:3, the distribution area of *G. uralensis* was identified by the RF algorithm, and its accuracy was verified.

Table 4. Classification accuracy of *G. uralensis* distribution areas under the GUVI model

Years	OA（%）	KC	*G. uralensis* UA（%）	*G. uralensis* PA（%）
2014	96.83	95.78	100	75
2015	95.8	94.73	100	100
2016	97.97	97.08	96.72	77.63
2017	95.44	94.03	97.25	92.19
2018	93.34	90.92	88.41	95.87
2019	89.91	87.95	74.31	91.85

2020	89.72	87.16	89.22	99.27
2021	90.72	89.21	69.47	71.08
2022	93	81.38	97.26	97.32

The classification accuracies of *G. uralensis* distribution areas under the GUVI model for 2014-2022 are shown in Table 4. The lowest value was 89.72% for OA, 81.38 for *KC* value, 69.47% for *G. uralensis* UA and 71.08% for *G. uralensis* PA. Therefore, the overall classification accuracy and individual classification accuracy of *G. uralensis* were satisfactory for 2014-2022 and can be used for *G. uralensis* range extraction.

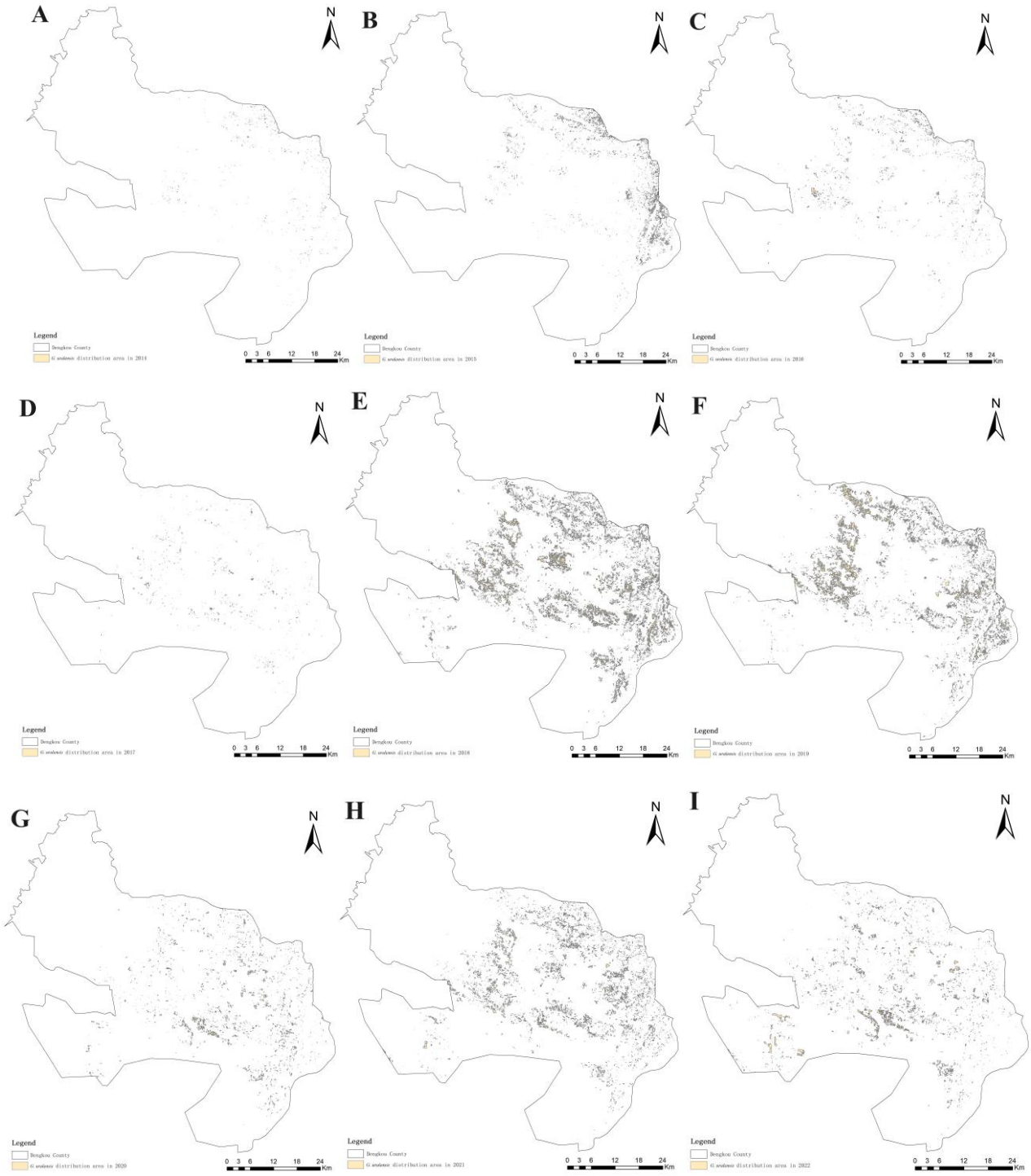


Figure 2. The distribution area of *G. uralensis* in Dengkou County from 2014 to 2022: A-I correspond to the years from 2014 to 2022 respectively

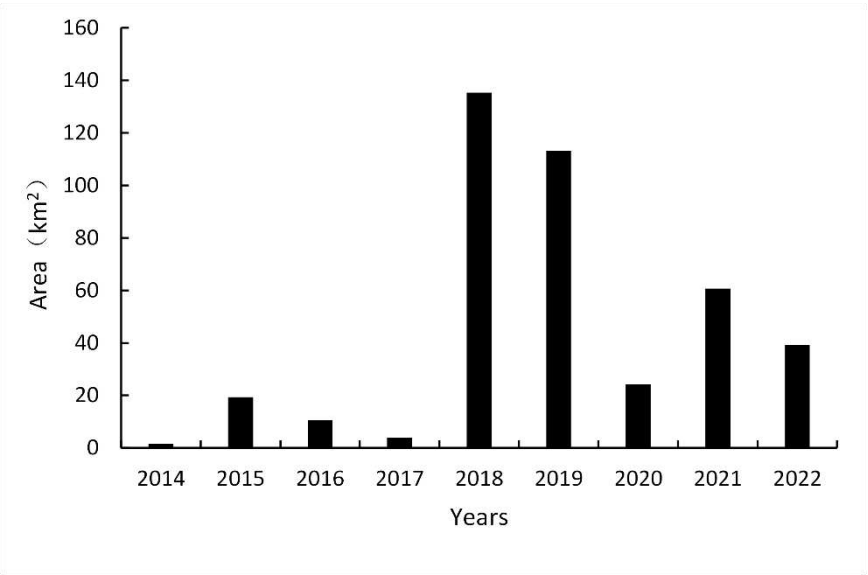


Figure 3. The dynamic alterations of the acreage of *G. uralensis* in Dengkou County during 2014-2022

The spatial distribution and area change of the *G. uralensis* distribution area from 2014 to 2022, extracted from the identification results of the *G. uralensis* distribution area using the RF algorithm under the GUVI model, are shown in Figures 2 and 3. As depicted in Figure 2, the distribution of *G. uralensis* has gradually expanded from its initial main concentration in the northeast of Dengkou County to the central region, and even now extends to the southwest. Its distribution area has also gradually transformed from being small and scattered initially to a large, concentrated distribution area. Figure 3, on the other hand, demonstrates the trend of *G. uralensis* area, which shows an increase and then a decrease, increasing from an initial fluctuation of 1.25 km^2 to 119.24 km^2, and then gradually reaching a plateau of 66.74-62.08km^2. Among them, the increase of *G. uralensis* area in 2018 was the most significant, which increased by 104.70 km^2 compared to the previous year. It can be observed that, since *G. uralensis* is a perennial plant, it is difficult to systematically count the area of *G. uralensis* planting and harvesting each year. However, it largely exhibits a stable planting pattern. Additionally, although Dengkou County has a long history of *G. uralensis* planting, the planting area was small before 2018, and only after 2018 did large-scale and extensive planting commence, which was a response to the surge in market demand for *G. uralensis*.

3.2. Validation of NPP in the G. uralensis range

The estimated values of the model are affected by a variety of factors, and there exists a certain error between them and the measured values. Therefore, it is of utmost importance to verify the accuracy of the model estimation results. In this study, the MODIS data product MOD17A3HGF NPP data was selected for comparison with the CASA model estimation result data used in this study. ArcMap software was utilized to extract the annual mean values of the MODIS NPP and the NPP estimated by the CASA model at the same point, and the R^2 and RMSE of the two groups of data were calculated for the comparative test to examine the linear relationship and the degree of dispersion of the two data sets. The results are presented in Figure 4 and Table 5. From Figure 4, it can be seen that the linear relationship between the CASA model estimates and the MODIS NPP values is good and passes the significance test ($p<0.01$), and the R^2 ranges from 0.682-0.9557, which indicates that there is a significant correlation between the two sets of data. According to Table 5, the RMSE is between 6.865739-17.666376, which indicates that the

two groups of data have fewer outliers, smaller deviations, and lower dispersion. Therefore, the results of the two data sets are more consistent, and the estimation of NPP in Dengkou County using CASA model has high credibility, and the simulation results can be used to conduct relevant research and analysis.

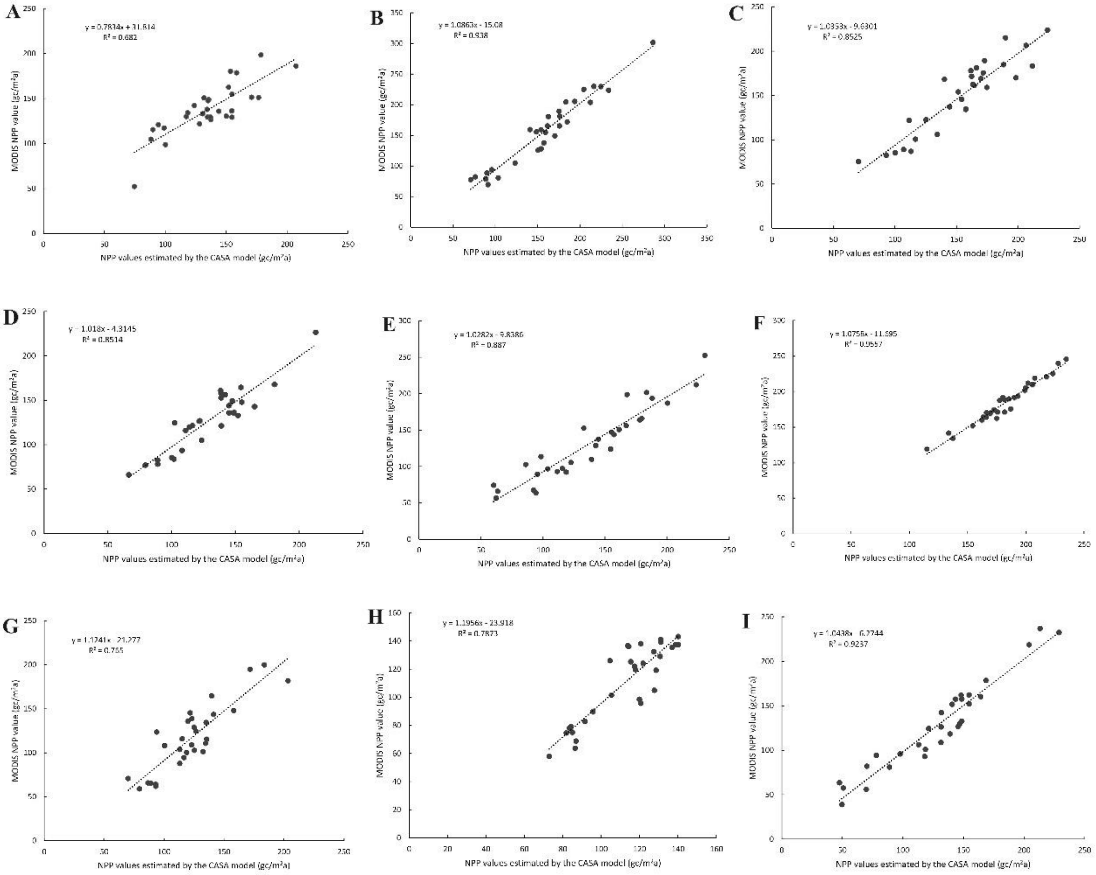


Figure 4. Relationship of CASA NPP estimates and MODIS NPP values in Dengkou County from 2014 to 2022: A-I correspond to the years from 2014 to 2022 respectively

Table 5. CASA NPP estimates and MODIS NPP validation results for Dengkou County during 2014-2022

Evaluation indicators	2014	2015	2016	2017	2018	2019	2020	2021	2022
R^2	0.682	0.938	0.8525	0.8514	0.887	0.9557	0.765	0.7873	0.9237
RMSE	17.05357	14.73133	16.23154	13.19273	17.66376	6.865739	19.51363	13.15288	13.65732

3.3. Spatial and temporal changes in NPP in the G. uralensis range

The changes in the annual mean values of NPP of *G. uralensis* in Dengkou County from 2014 to 2022 estimated using the CASA model are shown in Figure 5. The 2014-2022 NPP of *G. uralensis* in Dengkou County ranged from 556.119 to 791.587 gC/m² with a general decreasing trend and a maximum fluctuation of 235.468 gC/m². Compared with 2014, the annual mean NPP in Dengkou County in 2022 decreased by 75.27 gC/m². The highest value occurred in 2017 at 791.587 gC/m², which was higher than the overall 9-year average of about 125.8912 gC/m². There were three time points of significant reduction during the 9-year period, which were also 2015, 2019 and 2022, and the lowest annual mean NPP value was recorded in 2022 at 556.119 gC/m², which was lower than the overall 9-year average of 109.5768 gC/m².

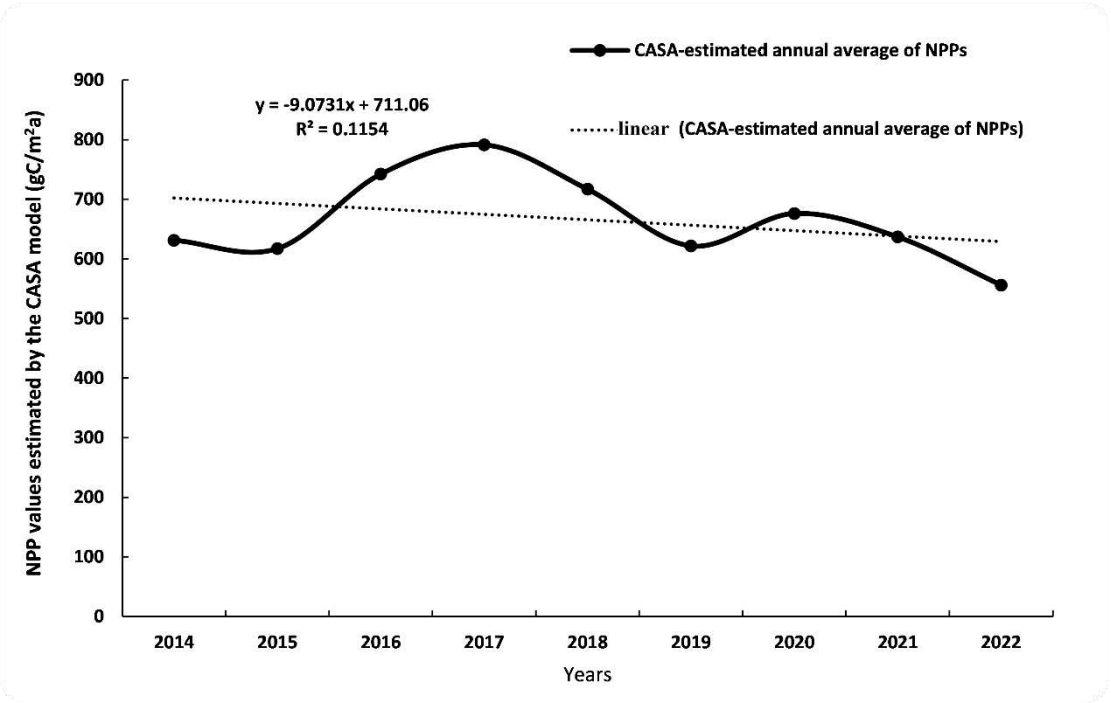
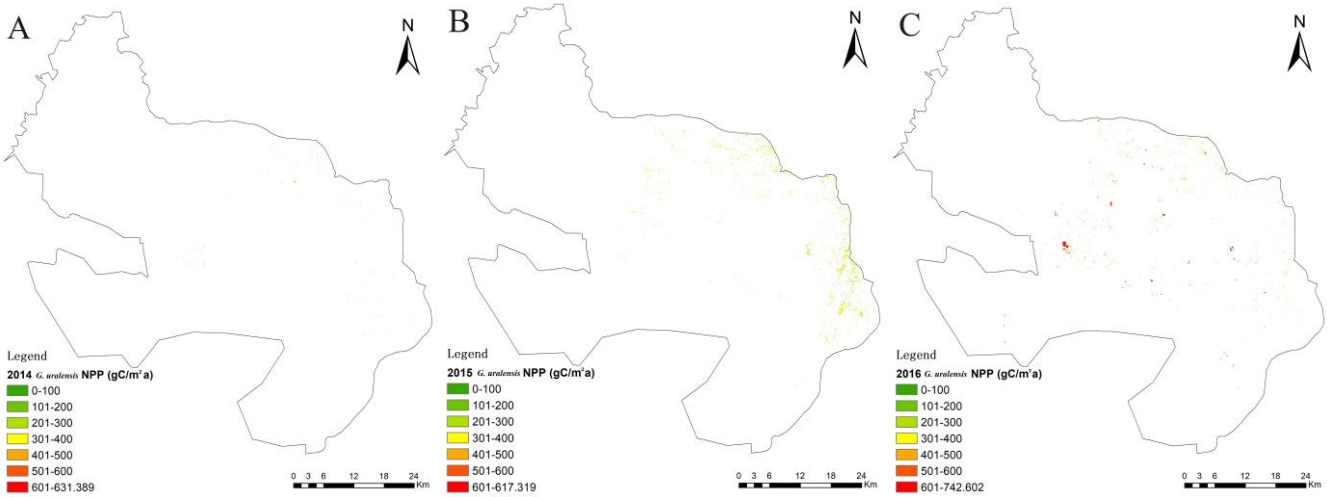


Figure 5. Change in annual average value of *G. uralensis* NPP in Dengkou County during 2014-2022

The NPP values estimated by the CASA model were classified into 7 classes using ArcMap software, and above 501 gC/m2 as the high value area, below 200 gC/m2 as the low value area, and 201-500 gC/m2 as the medium value area, which presented the spatial distribution results as shown in Figure 6. From Figure 6, it can be seen that the spatial distribution of annual mean value of *G. uralensis* NPP in Dengkou County varies greatly, and the low, medium and high value zones present uniform distribution characteristics and the value of *G. uralensis* NPP in the same location varies every year, which can be inferred that the carbon sequestration capacity of *G. uralensis* has a complex connection with the year and mode of *G. uralensis* planting and environmental factors.



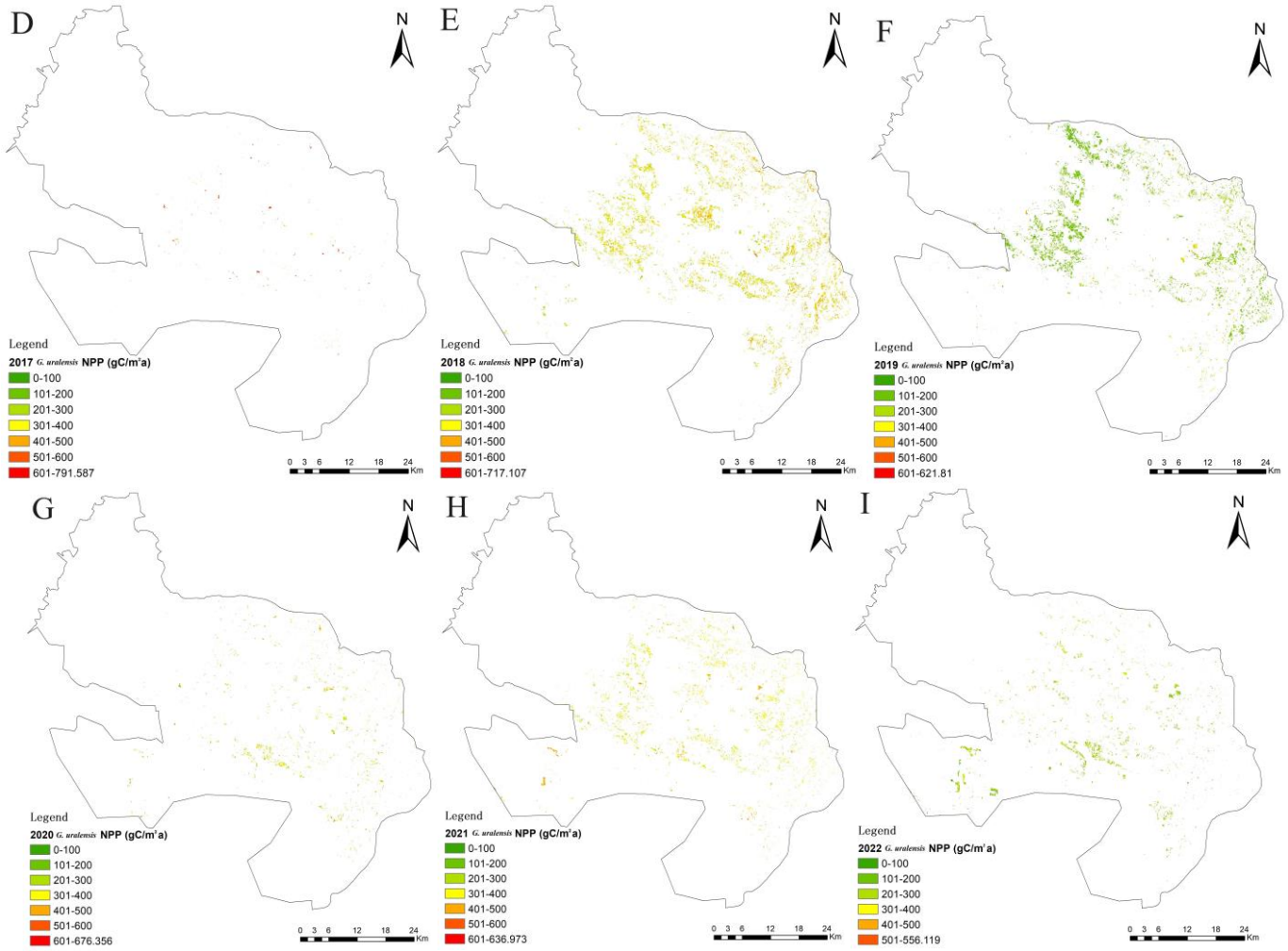


Figure 6. Spatial distribution of *G. uralensis* NPP values in Dengkou County from 2014 to 2022: A-I correspond to the years from 2014 to 2022 respectively

The statistics of the area share of low, medium, and high value zones of the annual mean value of NPP in the Dengkou County *G. uralensis* distribution area from 2014 to 2022 are shown in Table 6. The annual mean value of NPP of *G. uralensis* in Dengkou County during the period of 2014-2022, except for the year of 2019, shows that the area share of the medium value zone was significantly higher than that of the low and high value zones in the other years. In order to conduct a more comprehensive analysis of the carbon sequestration capacity of *G. uralensis* in Dengkou County during 2014-2022, the proportions of the area of the low value zone, the medium value zone, and the high value zone of the annual mean of *G. uralensis* NPP in Dengkou County relative to the annual mean of NPP in Dengkou County were examined, and the results are presented in Table 7. From the data in Table 7, it was found that the proportion of the low value area in the annual mean of *G. uralensis* NPP was relatively low, with an average value of 0.39%, and the proportion even dropped to 0 in 2014 and 2017. The average value of the proportion of the medium value area was 4.06%, which was slightly higher than that of the low value area but still at a relatively low level overall. In contrast, the share of the high value zone is significantly higher than the other two zones, with a mean value of 12.48% and even reaching as high as 52.94% in some years. At the same time, the total area of the *G. uralensis* distribution area in the overall area of Dengkou County is not large, with an average value of only 1.23%, and the highest value occupies only 3.68%. It can be observed that although the distribution area of *G. uralensis* is limited, its proportion in the high value area is relatively high, indicating that *G. uralensis* has a higher annual mean NPP value and a stronger carbon sequestration capacity compared with other feature types.

Table 6. *G. uralensis* NPP grade area share in Dengkou County during 2014-2022

Area	2014	2015	2016	2017	2018	2019	2020	2021	2022
low value area	0.203%	2.946%	1.316%	0.607%	6.997%	70.063%	19.650%	2.742%	37.576%
medium value area	94.476%	97.030%	65.670%	57.546%	91.118%	29.432%	77.822%	95.332%	62.393%
high value area	5.321%	0.024%	33.014%	41.847%	1.885%	0.506%	2.529%	1.926%	0.031%

Table 7. *G. uralensis* NPP class area share of NPP in Dengkou County during 2014-2022

Area	2014	2015	2016	2017	2018	2019	2020	2021	2022	average
low value area	0.00%	0.02%	0.01%	0.00%	0.38%	2.38%	0.17%	0.07%	0.45%	0.39%
medium value area	0.10%	2.21%	0.58%	0.21%	10.93%	9.43%	2.23%	5.05%	5.82%	4.06%
high value area	0.14%	0.10%	9.91%	5.74%	6.12%	52.94%	16.13%	14.05%	7.18%	12.48%
total area	0.04%	0.53%	0.29%	0.11%	3.68%	3.07%	0.66%	1.65%	1.07%	1.23%

3.4.Analysis of factors influencing spatial variation in NPP of G. uralensis

The effect of each environmental factor with the value of NPP of *G. uralensis* in Dengkou County in 2014-2022 was analyzed by factor detection in Geodetector, which reveals the magnitude of the effect of each spatial distribution of *G. uralensis* NPP in Dengkou County in 2014-2022. For the convenience of understanding, the results of the first 6 of the q value average of factor detection are shown in Table 8, and the detailed results can be seen in Table S 1. From Table 8, it can be seen that the q value of factors affecting the NPP of *G. uralensis* in Dengkou County in the years of 2014-2022 varies significantly. According to the size of the mean value of q value of the major categories of environmental factors in the order of climate type factor > terrain factor > soil factor > vegetation type factor. According to the average q value of each factor in 2014-2022, it can be seen that in 2014-2022, the influence of Dengkou County *G. uralensis* NPP is mainly affected by the monthly average sunshine duration factor of the climate type factor. during 2014-2022, the average q value of the average sunshine duration factor is the highest in August at 9.254; and the lowest mean value of q value of April mean sunshine duration factor was 0.8793. It indicated that the broad category of climate type factors had the greatest influence on the NPP of *G. uralensis* in Dengkou County during 2014-2022, and the single factor of August mean sunshine duration single factor had the greatest influence on the NPP of *G. uralensis* in Dengkou County during 2014-2022.

Table 8. Partial results of factor detection of spatial distribution of *G. uralensis* NPP and environmental factors during 2014-2022

Factor	2014	2015	2016	2017	2018	2019	2020	2021	2022	average
x60	0.8342	0.9502	0.9512	0.8911	0.9964	0.9728	0.9706	0.881	0.881	0.9254
x61	0.8342	0.9502	0.9442	0.8921	0.925	0.9744	0.986	0.885	0.885	0.9196
x57	0.8298	0.9469	0.9511	0.8855	0.942	0.9737	0.9631	0.8847	0.8847	0.9179
x58	0.8102	0.9374	0.9504	0.8921	0.98	0.9861	0.9866	0.8547	0.8547	0.9169
x53	0.8269	0.9452	0.9512	0.8223	0.9711	0.9814	0.9767	0.885	0.885	0.9161
x49	0.8311	0.9502	0.8631	0.8919	0.985	0.9673	0.9715	0.8834	0.8834	0.9141

Spatial distribution of *G. uralensis* NPP is the result of the interaction and combined influence of multiple factors. The interaction detection in the GeoDetector can be utilized to understand whether the effect of two environmental factors on the spatial distribution of *G. uralensis* NPP is weakened, enhanced, or independent. Given the large number of factors used in this study, the

interaction and ecological detection results of the top six factors in each year are primarily presented in the paper, while the interaction and ecological detection results of all factors can be found in Table S 2.

As can be observed from Table 9, most of the interaction q values of the factors with the top 6 q values of the factor detection results for each year were greater than the q values of the single factors. The interaction was dominated by two-factor enhancement, followed by one-factor nonlinear attenuation, and then nonlinear enhancement. The highest q values for the period 2014-2022 were 0.8359, 0.9507, 0.9517, 0.8931, 0.9974, 0.9862, 0.9868, 0.8861, and 0.8861, and most of them are two-factor enhancement. This indicates that the effects of each environmental spatial distribution of *G. uralensis* NPP do not exist in isolation but are part of a complex and close interaction relationship.

Table 9. Partial results of interaction detection of spatial distribution of *G. uralensis* NPP with environmental factors during 2014-2022

Years	**Factor**						
		x49	x55	x57	x60	x61	x62
2014	x49	0.8311	c	c	c	c	c
	x55	0.8359	0.8342	c	c	c	c
	x57	0.8359	0.8359	0.8298	c	c	c
	x60	0.8359	0.8359	0.8359	0.8342	c	c
	x61	0.8359	0.8359	0.8359	0.8359	0.8342	c
	x62	0.8359	0.8359	0.8359	0.8359	0.8359	0.8331
2015		x49	x51	x55	x60	x61	x62
	x49	0.9502	e	b	b	b	b
	x51	0.9507	0.9499	b	b	b	c
	x55	0.9507	0.9507	0.9502	c	c	c
	x60	0.9507	0.9507	0.9507	0.9502	c	c
	x61	0.9507	0.9507	0.9507	0.9507	0.9502	c
	x62	0.9507	0.9507	0.9507	0.9507	0.9507	0.9491
2016		x50	x53	x55	x57	x60	x62
	x50	0.9512	c	c	c	c	c
	x53	0.9517	0.9512	c	c	c	c
	x55	0.9517	0.9517	0.9512	c	c	c
	x57	0.9517	0.9517	0.9517	0.9511	c	c
	x60	0.9517	0.9517	0.9517	0.9517	0.9512	c
	x62	0.9517	0.9517	0.9517	0.9517	0.9517	0.9512
2017		x49	x54	x58	x60	x61	x62
	x49	0.8919	c	c	c	c	c
	x54	0.8931	0.8921	c	c	c	c
	x58	0.8931	0.8931	0.8921	c	c	c
	x60	0.8931	0.8931	0.8931	0.8911	c	c
	x61	0.8931	0.8931	0.8931	0.8931	0.8921	c
	x62	0.8931	0.8931	0.8931	0.8931	0.8931	0.8913
2018		x54	x55	x56	x59	x60	x62
	x54	0.9940	c	c	c	c	c
	x55	0.9974	0.9965	c	c	c	c
	x56	0.9974	0.9974	0.9973	c	c	c
	x59	0.9974	0.9974	0.9974	0.9937	c	c
	x60	0.9974	0.9974	0.9974	0.9974	0.9964	c
	x62	0.9974	0.9974	0.9974	0.9974	0.9974	0.9970
2019		x50	x53	x55	x56	x58	x62
	x50	0.9861	c	c	c	c	c

Years	Factor					
	x53	0.9862	0.9814	c	c	c	c
	x55	0.9862	0.9862	0.9861	c	c	c
	x56	0.9862	0.9862	0.9862	0.9827	c	c
	x58	0.9862	0.9862	0.9862	0.9862	0.9861	c
	x62	0.9862	0.9862	0.9862	0.9862	0.9862	0.9854
		x49	x53	x54	x58	x60	x61
	x49	0.9715	c	c	c	c	c
	x53	0.9868	0.9767	c	c	c	c
2020	x54	0.9868	0.9868	0.9866	c	c	c
	x58	0.9868	0.9868	0.9868	0.9866	c	c
	x60	0.9868	0.9868	0.9868	0.9868	0.9706	c
	x61	0.9868	0.9868	0.9868	0.9868	0.9868	0.9860
		x49	x53	x57	x59	x60	x61
	x49	0.8834	c	c	c	c	c
	x53	0.8861	0.8850	c	c	c	c
2021	x57	0.8861	0.8861	0.8847	c	c	c
	x59	0.8861	0.8861	0.8861	0.8840	c	c
	x60	0.8861	0.8861	0.8861	0.8861	0.8810	c
	x61	0.8861	0.8861	0.8861	0.8861	0.8861	0.8850
		x49	x53	x57	x59	x60	x61
	x49	0.8834	c	c	c	c	c
	x53	0.8861	0.8850	c	c	c	c
2022	x57	0.8861	0.8861	0.8847	c	c	c
	x59	0.8861	0.8861	0.8861	0.8840	c	c
	x60	0.8861	0.8861	0.8861	0.8861	0.8810	c
	x61	0.8861	0.8861	0.8861	0.8861	0.8861	0.8850

* In the table, b is Weaken, ni-, c is Enhance, bi-, and e is Enhance, nonlinear.

The ecological detector of the GeoDetector was primarily employed to compare whether there was a significant difference between the effects of the two factors on the spatial distribution of *G. uralensis* NPP. If there is a significant difference between the effects of two factors on the spatial differentiation of *G. uralensis* NPP, it is marked as "Y", and if there is no significant difference, it is marked as "N". From the results (in Table S 3.), it can be seen that there was no significant difference in the spatial distribution of *G. uralensis* NPP between most of the influencing factors, and only a very few influencing factors had a significant difference in the spatial distribution of *G. uralensis* NPP between the same factor and the same factor. It can be observed that the interactions among environmental factors are highly complex, and the effects of two factors with higher q values on the spatial distribution of *G. uralensis* NPP are different, and the effects of the same factors on the spatial distribution of *G. uralensis* NPP in different years are also different.

4. Discussion

4.1. Spatial and temporal changes in the distribution area of G. uralensis

Dengkou County belongs to the (semi-)arid region, and its ecological environment is fragile. Coupled with unreasonable human activities, the ecosystem services have been severely affected. As the upstream area of the Yellow River Basin, the ecosystem of the Yellow River Basin exhibits a holistic and public nature of service functions, and the firm ecological security barrier in the upstream of the Yellow River influences the development of the downstream region and even the entire country. *G. uralensis* holds great economic value due to its medicinal properties, and its well-developed root system plays an

important role in (semi-)arid areas, such as in ecological protection, windbreak, and sand fixation. It possesses significant economic and ecological values for improving the economic development and ecological environment of (semi-)arid areas. During the period from 2014 to 2022, the distribution area of *G. uralensis* in Dengkou County underwent significant changes. Initially, the *G. uralensis* distribution area was mainly concentrated in the northeastern part, and subsequently, it gradually expanded to the central and southwestern parts of the county, resulting in a large and concentrated distribution. Its area initially fluctuated around 1.25 km² and then increased to 119.24 km², after which it gradually stabilized within the range of 66.74-62.08 km².

This study indicates that both natural conditions and anthropogenic factors have contributed to this change. Firstly, the northeastern part of Dengkou County, which is nourished by the Yellow River, has abundant water resources. As a perennial plant, *G. uralensis* has a high water demand. Therefore, the northeastern region, with the advantage of Yellow River irrigation, provides unique conditions for the growth of *G. uralensis*. Growers are inclined to cultivate *G. uralensis* in this area taking advantage of this benefit. Secondly, as the medicinal value of *G. uralensis* is gradually gaining wider recognition, the market demand is growing. To meet this demand, the cultivation of *G. uralensis* has gradually expanded, thus extending from the northeast to the center and southwest, that is, in 2014-2016. *G. uralensis* demonstrates greater adaptability to soil conditions and is capable of growing in a wide range of soil types. This adaptability provides the possibility of cultivating it in a wider area, resulting in turn has led to a large and concentrated distribution, especially during 2017 - 2020, the area expanded from 13.20 km² to 119.24 km². In addition, this study suggests that the changes in *G. uralensis* distribution are not the result of entirely natural evolution. Anthropogenic factors have played an important role in driving these changes. The local agricultural technology extension department may have provided training and guidance on *G. uralensis* cultivation techniques, which improved farmers' cultivation skills and management levels. Simultaneously, with the large-scale development of the *G. uralensis* plantation industry, the cooperation and exchange among growers have become more frequent. Through sharing planting experiences and optimizing the planting mode, etc., the efficiency and competitiveness of *G. uralensis* plantation have been further enhanced, promoting the cumulative and centralized distribution over a large area. However, the cultivation area of *G. uralensis* shows obvious fluctuating changes during 2014-2022. This may be the result of a combination of factors, such as growers' inconsistent harvesting years and intensified market competition, which may have led some growers to adjust their *G. uralensis* planting areas. In summary, the change in the *G. uralensis* distribution area in Dengkou County is the result of the combined action of natural conditions and human factors. In the future, to promote the sustainable development of *G. uralensis* plantations, it is necessary to continue to pay attention to and study the growth characteristics and market demand of *G. uralensis* and seek reasonable planting strategies to achieve sustainable development.

4.2. Spatial and temporal changes in NPP in the G. uralensis range

The changes in the annual mean value of NPP in the *G. uralensis* distribution area in Dengkou County from 2014 to 2022 generally exhibited a fluctuating downward trend. Regarding natural factors, Dengkou County might have experienced unfavorable climatic conditions, such as increasing temperature and decreasing precipitation during these years, which affected the growth and photosynthesis of vegetation; alternatively, natural disasters, including diseases and pests, could have led to the damage of vegetation, thereby influencing the annual mean value of NPP. With respect to the human factor, more *G. uralensis* might have been harvested than planted during these years, resulting in a significant decrease in the annual mean value of NPP. From the perspective of

systematic error, there could have been some errors or biases in data processing and statistical methods, leading to the fluctuating downward trend in the annual average value of NPP. In terms of spatial variation, the spatial distribution of the annual mean values of NPP of *G. uralensis* in Dengkou County varied significantly. When analyzing the natural factors, there were annual variations in climatic factors, such as precipitation, temperature, and light, directly affected the physiological processes of *G. uralensis*, including photosynthesis, respiration, and nutrient uptake, thus leading to the changes in NPP. Meanwhile, soil nutrient content, soil moisture status, and soil texture also vary with seasons and years, and these factors also affect the growth of *G. uralensis* and NPP values. Anthropogenic factors, such as agricultural management practices and land use practices, also affect the NPP of *G. uralensis*.

The low, medium, and high annual mean NPP values of *G. uralensis* in Dengkou County during the period 2014-2022 were found to be less variable in all years except 2019. In addition, it was found that the distribution area of *G. uralensis* accounted for a smaller proportion in the low and medium value zones of the Dengkou County NPP annual mean and a larger proportion in the high value zone, which indicates that *G. uralensis* has a strong carbon sequestration capacity. In addition, Zhang [42] calculated the carbon sequestration of two crops, *Z. mays* and *Triticum aestivum* L., in the Fen River Basin from 2011 to 2020. Their average total carbon sequestration values were 368.65 gC/m² and 333.49 gC/m², respectively. In contrast, the *G. uralensis* in this study exhibited a significant carbon sequestration advantage, with an average total carbon sequestration value ranging from 556.119 to 791.587 gC/m², which was approximately 1.67 - 1.98 times higher than that of traditional crops. *G. uralensis* also shows significant advantages in the field of ecological restoration. To investigate the restoration of desert soils in arid mining areas by different vegetation, Long et al. [43]selected the South Lake No. 2 mining area in Hami, Xinjiang, as the research object and examined the effects of seven vegetation types on the physicochemical properties of the soil and the growth of the vegetation. After analyzing and testing soil physicochemical indexes such as total nitrogen, total phosphorus, and total potassium of these plants, it was found that *Medicago sativa* L., *G. uralensis*, and *Haloxylon ammodendron* (C. A. Mey.) Bunge were the preferred plants regarding ecological restoration benefits. The above-mentioned study fully demonstrated that compared with traditional crops, *G. uralensis* not only has a stronger carbon-fixation capacity but also has significant advantages in the ecological restoration of arid mining areas. However, its ecological adaptability and sustainability still need to be considered in practical application. Overexploitation or irrational use may lead to the depletion of *G. uralensis* resources or the destruction of the ecological environment, which in turn may affect its carbon sequestration capacity. Therefore, when utilizing *G. uralensis* for carbon sequestration, it is necessary to formulate reasonable development strategies and management measures to ensure the sustainable utilization of its resources and the stability of the ecological environment. As a potential plant for carbon sequestration, *G. uralensis* is worthy of further research and utilization in future carbon reduction and ecological restoration.

4.3. Effects of environmental factors on the spatial distribution of G. uralensis NPP

Based on the results of the GeoDetector, it can be observed that the NPP of *G. uralensis* in Dengkou County during the period from 2014 to 2022 is mainly influenced by climate type factors, followed by topographic factors, soil factors, vegetation type factors, and so on. Among the climate type factors, temperature, precipitation, and sunshine duration factors have particularly significant impacts on NPP, and they directly determine the efficiency of plant photosynthesis and the suitability of the growing environment. Specifically, suitable temperature can promote the activity of plant enzymes and increase the rate of photosynthesis. Sufficient precipitation can ensure the normal water demand of plants,

which is conducive to their growth and development. Sunshine duration affects the time of photosynthesis in plants, and the longer the sunshine duration, the more organic substances are synthesized, thereby increasing the amount of NPP. In addition, changes in sunshine duration in different months affect the growth cycle and growth state of plants. In months with longer sunshine duration, the photosynthetic capacity of plants is enhanced, and their growth rate is accelerated, which is conducive to the accumulation of NPP. Therefore, it is reasonable that climate type factors have the greatest influence on NPP, as they provide the necessary conditions for plant growth and material accumulation.

The influence of terrain factors, soil factors, and vegetation type factors on NPP is also non-negligible. However, the GeoDetector results indicate that these factors have less influence on the NPP of *G. uralensis* in Dengkou County, mainly due to the relatively homogeneous topography, soil, and vegetation type of the area, which weakens the impact of these factors on the spatial distribution of *G. uralensis* NPP. Specifically, the distribution area of *G. uralensis* in Dengkou County is mainly located in the Hetao Plain area, which has a flat and open topography and lacks significant topographic variations. As a result, topographic factors such as elevation, slope, and slope direction exhibit less variability in the area and relatively less influence on the NPP of *G. uralensis*. Soil factors have similarly limited influence in the *G. uralensis* growing area of Dengkou County. Due to the relative homogeneity of soil types in the area, soil factors such as soil organic carbon, texture, and effective moisture content have a limited range of variability. Therefore, the influence of soil factors on *G. uralensis* growth and NPP is not as significant as that of climatic factors. Finally, although Dengkou County is rich in vegetation types, *G. uralensis* distribution areas are mainly located in agricultural land areas, which are predominantly managed and cultivated by humans and are surrounded by fewer tall plants competing with *G. uralensis* for sunlight and nutrients. Therefore, the vegetation type factor also has less influence on the NPP of *G. uralensis* in Dengkou County.

In actual ecosystems, factors do not function in isolation but are interrelated and interact with one another, and together they form an intricate network that synergistically regulates NPP production and changes. Although the present study found that the effects of topography, soil, and vegetation type factors on *G. uralensis* NPP were relatively small in the particular region of Dengkou County, this does not imply that the effects of these factors can be readily ignored in other regions. Different regions possess different ecological environments, and there may be significant differences in these factors, which may affect NPP to varying degrees. Therefore, when studying NPP in different regions, it is still necessary to comprehensively consider the combined effects of multiple factors in order to more accurately reveal the mechanism of NPP change and its relationship with environmental factors.

5. Conclusion

With climate change and irrational human activities, the ecosystems of (semi-)arid regions are deteriorating. The search for solutions with prospects for ecological restoration and economic development has become an important consideration. The cultivation of medicinal plants is one of the important sources of income for farmers. However, both farmers and scholars tend to focus excessively on their economic value and relatively neglect their ecological value. In the current context of a deteriorating ecological environment, there is an urgent need to seek an economic and ecological win-win strategy to alleviate the pressure brought by climate change. In this study, we selected *G. uralensis*, a leguminous plant with high economic value and carbon sequestration capacity, as the research object, and Dengkou County, which has rich planting experience and a long planting history, as the study area. We explored the carbon sequestration capacity of *G.*

uralensis and its influencing factors in depth through long time series data analyses. Firstly, the study identified and extracted the distribution areas of *G. uralensis* from remote sensing images from 2014 to 2022using the RF algorithm based on the spectral characteristics of *G. uralensis* within the vegetation index model of *G. uralensis* for major feature types in different years. It was found that the distribution of *G. uralensis* gradually expanded from its initial main concentration in the northeastern part of Dengkou County to the central region and even to the southwestern part. Its distribution area also changed from being small and scattered initially to being large and concentrated. Subsequently, the improved CASA model was used to estimate the annual mean value of NPP of *G. uralensis* in Dengkou County from 2014 to 2022 and to analyze its temporal and spatial changes. The results showed a general fluctuating and decreasing trend of the NPP annual mean values in *G. uralensis* distribution areas. The spatial distribution of the NPP annual mean values of *G. uralensis* in Dengkou County varied significantly, and the low and medium value areas accounted for a smaller proportion while the high value areas accounted for a larger proportion in the Dengkou County NPP annual mean values, which further proved that *G. uralensis* had a high carbon sequestration capacity. Finally, the relationship between the annual mean NPP of *G. uralensis* and 71 environmental factors in Dengkou County from 2014 to 2022 was analyzed using a GeoDetector. It was found that the distribution of *G. uralensis* was mainly influenced by the climate type factor, followed by the topographic factor, soil factor, and vegetation type factor. In the single factor analysis, the effect of average sunshine duration on the NPP of *G. uralensis* in Dengkou County was particularly significant. In addition, the effects of each environmental factor on *G. uralensis* NPP did not exist independently but had a complex interaction relationship. Therefore, through rational cultivation of *G. uralensis*, not only can the local economy be driven and the income level of residents be improved, but it can also provide an important reference basis for ecological restoration, desert management, and the rational layout of the carbon sequestration system in arid and semi-arid areas. Through in-depth research and rational utilization of the ecological and economic value of *G. uralensis*, it is expected to achieve economic development while effectively protecting and improving the ecological environment.

There are still several shortcomings in this study. Firstly, MODIS NPP data were utilized in this study for comparison and validation with the estimated NPP results. However, performing the comparison and validation with real field data could more accurately uncover the possible errors and biases of the improved CASA model combined with the GF-1 WFV remote sensing imagery in the estimation of NPP. Additionally, only environmental factors were incorporated into the study of the relationship between NPP and impact factors of *G. uralensis* in Dengkou County, and human factors were not included. Therefore, it is necessary to collect as many human factors as possible for the analysis of impact factors in the future.

Author Contributions: Conceptualization, X.Z., S.S., M.L. and T.S.; methodology, X.W.; software, T.S.; validation, X.W., Z.Z. and T.C.; formal analysis, X.W.; investigation, S.S., M.L. and T.S.; resources, X.W., Z.Z. and T.C.; data curation, X.W., Z.Z. and T.C.; writing—original draft preparation, X.W.; writing—review and editing, X.Z., S.S., M.L. and T.S.; visualization, X.Z., X.W., Z.Z. and T.C.; supervision, S.S., M.L. and T.S.; project administration, S.S., M.L. and T.S.; funding acquisition, S.S., M.L. and T.S. All authors have read and agreed to the published version of the manuscript.

Funding: This study was supported by the Scientific and technological innovation project of China Academy of Chinese Medical Sciences（CI2021A03902, CICI2021B013）, the Fundamental Research Funds for National Natural Science Foundation of China （M2342002）, Independent research projects of Inner Mongolia University and Central Public Welfare Research Institutes under Grant ZZXT202313, ZZXT202406 and ZZ14-YQ-045.

Data Availability Statement: Data is provided within the manuscript or supplementary information files. For more details, please contact the author Xinxin Wei at weixinxin_im@163.com.

Conflicts of Interest: The authors declare no conflicts of interest.

Supplementary

Table S 1. Factor detection results of spatial distribution and environmental factors of *G. uralensis* NPP during 2014-2022

Table S 2. Results of interaction detection of spatial distribution of *G. uralensis* NPP with environmental factors during 2014-2022

Table S 3. Results of Ecological detection of spatial distribution of *G. uralensis* NPP with environmental factors during 2014-2022

References

[1] W. Chen, G. Wang, and J. Zeng, "Impact of urban expansion on ecosystem services in different urban agglomerations in China," *International Journal of Environmental Science and Technology,* vol. 20, no. 11, pp. 12625-12644, 2023.

[2] C. B. Field, M. K. v. Aalst, W. N. Adger *et al.*, "Part A: Global and Sectoral Aspects: Volume 1, Global and Sectoral Aspects: Working Group II Contribution to the Fifth Assessment Report of the Intergovernmental Panel on Climate Change."

[3] M. Ulyshen, and S. Horn, "Declines of bees and butterflies over 15 years in a forested landscape," *Current Biology,* vol. 33, no. 7, pp. 1346-+, Apr, 2023.

[4] W. P. Cramer, D. W. Kicklighter, A. Bondeau *et al.*, "Comparing global models of terrestrial net primary productivity (NPP): overview and key results," *Global Change Biology,* vol. 5, 1999.

[5] L. Cui, J. Shi, and Y. Ma, "A Comparison of Thermal Growing Season Indices for the Northern China during 1961–2015," *Advances in Meteorology,* vol. 2017, pp. 1-14, 2017.

[6] G. Yanjing, "Spatio-temporal dynamics of vegetation Net Primary Productivity Based on CASA Model: a case study of Bailongjiang watershed," bachelor's degree, Lanzhou University, 2015.

[7] H. Dandan, "Study on the spatiotemporal of NPP and its response to driving factors in Anhui province,China," bachelor's degree, Anhui Normal University, 2020.

[8] R. S. DeFries, C. B. Field, I. Y. Fung *et al.*, "Mapping the land surface for global atmosphere-biosphere models: Toward continuous distributions of vegetation's functional properties," *Journal of Geophysical Research,* vol. 100, pp. 20867-20882, 1995.

[9] R. Nijbroek, and S. J. Andelman, "Regional suitability for agricultural intensification: a spatial analysis of the Southern Agricultural Growth Corridor of Tanzania," *International Journal of Agricultural Sustainability,* vol. 14, pp. 231 - 247, 2016.

[10] L. M. Mungai, J. P. Messina, and S. S. Snapp, "Spatial Pattern of Agricultural Productivity Trends in Malawi," *Sustainability*, 2020.

[11] J. A. Aguirre-Liguori, S. Ramírez-Barahona, P. Tiffin *et al.*, "Climate change is predicted to disrupt patterns of local adaptation in wild and cultivated maize," *bioRxiv*, 2019.

[12] S. Savary, and L. Willocquet, "Modeling the Impact of Crop Diseases on Global Food Security," *Annual review of phytopathology*, 2020.

[13] P. Smith, K. V. Calvin, J. N. Nkem *et al.*, "Which practices co-deliver food security, climate change mitigation and adaptation, and combat land degradation and desertification?*," *Global Change Biology,* vol. 26, pp. 1532 - 1575, 2019.

[14] K. Edo, L. Kidane, and T. Beyene, "Socio-ecological Benefit of Homegarden Agroforestry and Their Indigenous Management System: A Case Study in Digelu Tijo District, Oromia, Ethiopia," *Momona Ethiopian Journal of Science*, 2024.

[15] P. Smith, "Carbon sequestration in croplands: The potential in Europe and the global context," *European Journal of Agronomy,* vol. 20, pp. 229-236, 2004.

[16] A. M. Toro, and E. Harsanyi, "What is the Connection between Soil Carbon Dioxide Emission, Global Warming and Food

Security?," *European Journal of Sustainable Development*, 2019.

[17] H. S. Ghazzawy, A. Bakr, A. T. Mansour *et al.*, "Paulownia trees as a sustainable solution for CO2 mitigation: assessing progress toward 2050 climate goals," *Frontiers in Environmental Science,* vol. 12, 2024-February-28, 2024.

[18] C. Gaolu, C. Lin, P. Danbo *et al.*, "Study on Carbon Sequestration and Oxygen Release Capacity of 10 Typical Plants in Helan Mountain," *Journal of Soil and Water Conservation,* vol. 35, no. 03, pp. 206-213+220, 2021.

[19] L. Andreu-Coll, M. Cano-Lamadrid, L. Noguera-Artiaga *et al.*, "Economic estimation of cactus pear production and its feasibility in Spain," *Trends in Food Science & Technology,* vol. 103, pp. 379-385, 2020/09/01/, 2020.

[20] C. Guobao, and Z. Jiarong, "Application of Licorice Products in Food," *China Food Safety Magazine*, no. 16, pp. 190-192, 2023.

[21] J. Kim, C.-S. Kim, Y. S. Kim *et al.*, "Jakyakgamcho-tang and Its Major Component, Paeonia Lactiflora, Exhibit Potent Anti-glycation Properties," *Journal of exercise nutrition & biochemistry,* vol. 20, no. 4, pp. 60-64, 2016 12, 2016.

[22] Y.-S. Park, S.-M. Kang, Y.-J. Kim *et al.*, "Exploring the dietary and therapeutic potential of licorice (Glycyrrhiza uralensis. Fisch.) sprouts," *Journal of ethnopharmacology,* vol. 328, pp. 118101, 2024 Mar 23 (Epub 2024 Mar, 2024.

[23] W. X. Xia, H. M. Zhang, M. X. Tao *et al.*, "Multi-omics techniques to compare the potential of raw and processed licorice as food supplements for ameliorating chronic fatigue syndrome," *Food Bioscience,* vol. 56, Dec, 2023.

[24] R. Q. Yang, and G. P. Zhao, "Inhibitory Effects of Glycyrrhiza Uralensis Fisch Extract on Cariogenic Virulence Factors of Streptococcus Mutans," *Indian Journal of Microbiology,* vol. 62, no. 3, pp. 473-473, Sep, 2022.

[25] C. Li, "Cultivation Technology of Licorice Planting for Desert Ecological Restoration and Governance," *Nongmin Zhifuzhiyou Yuekan*, no. 12, pp. 140, 2017.

[26] O. D. Akanbi, D. C. Bhuvanagiri, E. I. Barcelos *et al.*, "Integrating Multiscale Geospatial Analysis for Monitoring Crop Growth, Nutrient Distribution, and Hydrological Dynamics in Large-Scale Agricultural Systems," *Journal of Geovisualization and Spatial Analysis,* vol. 8, no. 1, Jun, 2024.

[27] S. Kartal, M. C. Iban, and A. Sekertekin, "Next-level vegetation health index forecasting: A ConvLSTM study using MODIS Time Series," *Environmental Science and Pollution Research*, 2024 Feb, 2024.

[28] B. Sisheber, M. Marshall, D. Mengistu *et al.*, "Assimilation of Earth Observation Data for Crop Yield Estimation in Smallholder Agricultural Systems," *Ieee Journal of Selected Topics in Applied Earth Observations and Remote Sensing,* vol. 17, pp. 557-572, 2024.

[29] Z. Le, and L. Lihua, "Solidly Promoting the Ecological Protection and High-Quality Development of the Yellow River Basin - Based on the Investigation and Research of Dengkou County, Bayannur City," *Industrial Innovation*, no. 21, pp. 24-26, 2022.

[30] J. Nuolin, H. Shuaiqi, L. Xinyi *et al.*, "Investigation on the Governance Status of Ulanbuh Desert Area in Dengkou County," *Haihe Water Resources*, no. S1, pp. 35-39, 2022.

[31] J.-Y. Yuan, L. Xiong, Z.-W. Wu *et al.*, "Characteristics of pine wood nematode disease in Nankang District, Ganzhou, Jiangxi Province, China," *Ying yong sheng tai xue bao = The journal of applied ecology,* vol. 35, no. 2, pp. 507-515, 2024, 2024.

[32] G. Qian, W. Jiahao, Z. Jian *et al.*, "Vegetable Recognition Based on Unmanned Aerial Vehicle （UAV） Multispectral Imagery and Random Forest Algorithm," *Journal of Agricultural Science and Technology,* vol. 25, no. 02, pp. 99-110, 2023.

[33] Y. Wu, Y. Feng, X. Xu *et al.*, "Scalability analysis of typical remote sensing image classification method," *Modern Electronics Technique,* vol. 47, no. 06, pp. 137-141, 2024.

[34] Z. Wenquan, P. Yaozhong, and Z. Jinshui, "ESTIMATION OF NET PRIMARY PRODUCTIVITY OF CHINESE TERRESTRIAL VEGETATION BASED ON REMOTE SENSING," *Chinese Journal of Plant Ecology*, no. 03, pp. 413-424, 2007.

[35] L. He, C. Li, Z. He *et al.*, "Evaluation and Validation of the Net Primary Productivity of the Zoigê Wetland Based on Grazing Coupled Remote Sensing Process Model," *IEEE Journal of Selected Topics in Applied Earth Observations and Remote Sensing,* vol. 15, pp. 440-447, 2022.

[36] X. Yifan, L. Yiu-lam, P. Bowen *et al.*, "Study on Estimation of Net Primary Productivity Based on High Resolution Remote Sensing Image and Its Influencing Factors in Yinchuan Cit," *Geomatics and Information Science of Wuhan University*, pp. 1-17, 2023.

[37] P. Fang, N. N. Yan, P. P. Wei *et al.*, "Aboveground Biomass Mapping of Crops Supported by Improved CASA Model and Sentinel-2 Multispectral Imagery," *Remote Sensing,* vol. 13, no. 14, Jul, 2021.

[38] J. Ke, D. D. Zhou, C. X. Hai *et al.*, "Temporal and Spatial Variation of Vegetation in Net Primary Productivity of the Shendong Coal Mining Area, Inner Mongolia Autonomous Region," *Sustainability,* vol. 14, no. 17, Sep, 2022.

[39] W. Jinfeng, and X. Chengdong, "Geo Detector: Principles and Prospects," *Acta Geographica Sinica,* vol. 72, no. 01, pp. 116-134, 2017.

[40] H. Junqi, bayhamwei, W. Jinquan *et al.*, "SpatialPatternsandDrivingFactorsofSoilNutrientContentsinCultivated LandsAcrossVariousTopographicalTypesintheLoessPlateau," *Research of Soil and Water Conservation*, pp. 1-11, 2024.

[41] Y. Zhou, T. Chen, J. J. Wang *et al.*, "Analyzing the Factors Driving the Changes of Ecosystem Service Value in the Liangzi Lake Basin-A GeoDetector-Based Application," *Sustainability,* vol. 15, no. 22, Nov, 2023.

[42] Z. Zhang, "Spatio-temporal simulation and analysis of crop net primary productivity based on CASA model," master's degree, Taiyuan University of Science and Technology, 2024.

[43] Y. Long, M. Wang, C. Huang *et al.*, " Different Vegetation Types Studied the Soil Restoration of the Hami Nanhu No.2 Coal Mine," *Tianjin Agricultural Sciences,* vol. 27, no. 03, pp. 80-85, 2021.

Supplementary Files

This is a list of supplementary files associated with this preprint. Click to download.

- Supplementary.zip